International Journal of GEOMATE
(Geotechnique, Construction Materials and Environment)
ISSN: 2186-2982 (P), 2186-2990 (O), Japan
Vol. 31, Issue 145, September 2026, PP. 47-56; DOI: 10.21660/2026.145.5601

IN-PLANE BEHAVIOR OF UNREINFORCED MASONRY (URM) WALLETTES WITH SELF-HEALING GEOPOLYMER MORTAR USING DIGITAL IMAGE CORRELATION (DIC)

*Albert A. Griño Jr[1] and Jason Maximino C. Ongpeng[2]

[1]Civil Engineering Department, Adamson University, Philippines; [2]Civil Engineering Department, De La Salle University, Philippines

*Corresponding Author, Received: 13 April 2026, Revised: 27 April 2026, Accepted: 07 May 2026

ABSTRACT: Geopolymer material is susceptible to cracking due to its inherent brittleness, which can compromise the service life of a structure. For that reason, the repair of these cracks is necessary and sometimes requires immediate attention. However, manually repairing the cracks takes a significant amount of time and resources. Hence, the self-healing of cracks is desirable to make maintenance and repair easier. This paper presents an experimental investigation of the in-plane behavior of unreinforced masonry wallettes with geopolymer and bacteria using digital image correlation (DIC). Moreover, it also aims to determine the strength contribution of the bacteria after pre-cracking the masonry wallette by 50% of the ultimate capacity. A two-dimensional (2D) Digital Image Correlation (DIC) technique was utilized in parallel with Linear Variable Differential Transformers (LVDT) to monitor the vertical deformation of the wallettes during testing and to capture the cracking of the unreinforced masonry wallette made of clay bricks. A percentage value difference of 17.09% was obtained from the vertical displacement of an unreinforced masonry wallette using the LVDT and DIC methods. Furthermore, it was demonstrated that incorporating bacteria with polypropylene fiber into an unreinforced brick wallette resulted in an ultimate shear stress of 2.77 MPa and a strength regain ratio of 225.39%. Thus, the experiment revealed that Digital Image Correlation (DIC) can be utilized as an alternate approach for evaluating the in-plane behavior of an unreinforced masonry wallette and that infusing bacteria and polypropylene fibers into a masonry wall can be a feasible alternative to strengthening the wall.

Keywords: Bacteria, Digital Image Correlation (DIC), Geopolymer mortar, Unreinforced masonry (URM) wallette, Polypropylene fiber

1. INTRODUCTION

Masonry walls are crucial structural elements that resist wind and earthquake loads, and their behavior under compression is brittle. Unreinforced masonry (URM) walls are typically designed to resist compression loads present in a structure with a little consideration to the forces generated from earthquake and impact loads. The behaviour of masonry structures under compression is brittle [1]. It is imperative that there is a need to retrofit and strengthen the masonry wall in a structure. To strengthen masonry structures, traditional techniques include surface treatment, grout and epoxy injections, externally bonded steel plates, and post tension. For the surface treatment and as an infill material in a structural member, cement mortar is the most used binder material in masonry construction, which can cause degradation over time because of the incompatibility issues.

An emerging alternative to cementitious materials is geopolymer, which can be synthesized by combining source materials rich in silica and alumina with strong alkali solutions. Fly-ash based geopolymer concrete exhibits similar structural behaviour to ordinary Portland cement (OPC) concrete [2]. Furthermore, geopolymers can provide better mechanical qualities, good durability in a range of chemical conditions, and strong resilience to increased temperatures, making them an ideal future substitute for traditional cement-based materials [3].

Geopolymer mortar are increasingly being explored as repair solutions for heritage structures since it is aligned with the principles of conservation philosophy which emphasize with the use of reversible and compatible materials for repair and restoration. One strategy for reducing costs and extending the lifetime of heritage structures is to use self-healing materials. A geopolymer mortar containing bacteria and polypropylene fiber is an innovative material with the ability to self-heal cracks. Thus, geopolymer composites reinforced with polypropylene fibers and bacteria are potential alternatives and applications for repair, retrofitting, and restoration in building construction.

A masonry wall is a composite structure built using bricks, concrete blocks, or stones bonded together using a cement mortar. It may be classified into reinforced, unreinforced, confined, and prestressed. Unreinforced masonry (URM) is the most common type of wall, typically used in historical buildings [4]. URM is a popular option due to its low cost, ease of construction, and reliance on local materials, making it a compelling choice for developing countries. Despite these advantages, a significant drawback exists. The majority of the URM structures were built without adhering to building codes and lacked proper structural detailing. This makes them vulnerable to damage even under low-intensity out-of-plane loads (lateral forces acting on the wall) [5]. To address this critical issue, developing effective retrofitting solutions for URM structures, especially unreinforced masonry walls, is essential.

Review of literature from highly cited journals revealed that unreinforced masonry (URM) walls are critically vulnerable to seismic loading, and researchers typically used a polymer-based (FRP) or mortar-based (TRM/FRCM). These fiber-based reinforcement methods have become a dominant approach to strengthen the wall structure over the past two decades. Glass fiber-reinforced polymer (GFRP) grids emerged as a popular reinforcement material, often evaluated through diagonal compression tests. Sisti et al. [6] compared three composites—GFRP grids, glass fiber nets, and polybenzoxazole cords—and concluded that GFRP grids offered superior performance based on load capacity and bonding characteristics. Similarly, Facconi et al. [7] observed a significant increase in maximum capacity (over 50% compared to the control) using alkali-resistant GFRP mesh for retrofitting. Righetti et al. [8] found that embedding GFRP grids in mortar can increase the load capacity of the wall panels. Liu et al. [9] demonstrated that GFRP can significantly enhance both flexural strength and deformation capacity of the walls relative to the unreinforced walls. Aside from GFRP, other reinforcement materials can also be used. Ferrara et al. [10] used flax textile as reinforcement and observed a substantial increase in load capacity of up to 136% with two layers of textile compared to unreinforced walls. Mustafaraj et al. [11] utilized polypropylene fibers and found a significant increase in the in-plane load capacity of up to 317% relative to unreinforced masonry walls. Recently, Junias and Nayak [12] considered polypropylene fibers as one of the internal strengthening materials in mortar in order to improve the impact resistance in masonry wall specimens. Finally, Elmalyh et al. [13] investigated the use of carbon fiber-reinforced polymer (CFRP) in URM walls, achieving an increase of up to 319% in compressive strength compared to control walls. These studies demonstrate various reinforcement materials that can be used for enhancing the performance of unreinforced masonry walls.

Unreinforced masonry (URM) structures are particularly susceptible to damage or collapse during earthquakes due to their brittle behavior [14]. These walls experience two main types of loading: in-plane (parallel to the wall surface) and out-of-plane (perpendicular to the wall surface). Studies by Brunner and Shing [15] suggest that URM walls failing due to diagonal cracking (in-plane shear) can exhibit higher capacity compared to those failing in flexure. Unreinforced masonry (URM) walls are vulnerable to several failure modes during seismic events, such as: (a) shear failure, (b) sliding failure, (c) rocking failure, and (d) toe crushing. These failure modes depend on the aspect ratio (aspect ratio = wall height/wall length), pre-existing compression (pre-compression), and the relative strength of the mortar joints compared to the masonry units (bond strength to compressive strength ratio). According to Nazir [16], walls with an aspect ratio less than 1 are more prone to shear failure (either base sliding or diagonal cracking), while walls with an aspect ratio greater than 1 are more likely to experience tensile uplift at the heel and crushing at the toe.

Unreinforced masonry (URM) buildings, a significant portion of the global building stock, often hold immense historical and cultural value [17]. In the Philippines, these structures serve as testaments to the country's rich heritage, exemplified by churches, watchtowers, and other landmarks scattered throughout the archipelago [18]. However, the masonry materials used in URM buildings—such as bricks, adobe, and stone—inevitably deteriorate over time. Repair, restoration, and strengthening become crucial for their preservation. Grout injection offers a valuable technique for addressing these challenges [19]. This method involves injecting a pressurized mixture of cement, sand, and water (grout) into cracks and voids within the masonry walls. The primary objective is to fill these gaps, effectively restoring the initial strength and functionality of the wall. For enhanced reinforcement, steel ties with mortar can be used to stitch cracks together, creating a more unified structure. The effectiveness of both grout injection and steel tie methods relies on achieving compatibility between the existing masonry and the repair materials. Compatibility in this context refers to ensuring that the physical and chemical properties of the new materials align with those of the original structure, thereby creating a unified system.

In recent years, the digital image correlation (DIC) technique has been used as an alternative technique to investigate the early crack propagation and deformation of a structural element in a structure. For this study, an optimal fly-ash based geopolymer mortar batch was chosen based on the ultimate compressive strength and strength regain percentages considering the different batches of geopolymer mortar produced. The optimized geopolymer batch was utilized as infill material in unreinforced masonry walletes. There has been no research into the utilization of a fly-ash-based geopolymer containing polypropylene fiber and bacteria as an infill material in unreinforced masonry walls cured at ambient temperature. The strength contribution of polypropylene fibers and bacteria to masonry walletes is investigated in this study by evaluating the changes in the diagonal shear strength and strength regain percentages of the unreinforced masonry wall. Moreover, Digital Image Correlation (DIC) using Ncorr software in Matlab was used to monitor the changes in the vertical displacement of the wallettes, and comparisons were made using the Linear Variable Displacement Transducer (LVDT) method.

2. RESEARCH SIGNIFICANCE

The present paper provides valuable insights about the potential of repairing the URM walls using geopolymer mortar with fiber and self healing bacteria. This offers a baseline reference for future researchers, engineers, and industry practitioners in the field of civil engineering. Moreover, it contributes to the existing knowledge about repair and strengthening methods of URM walls wherein conventional reinforcement would not be feasible to apply in a structure. The infill material made up of geopolymer mortar with polypropylene fibers and bacteria can be a promising solution to reduce the repair needs, extend the service life of a structure through self-healing, and lower the maintenance costs. Moreover, it highlights the potential use of digital image correlation (DIC) as a non-contact method to capture masonry behavior and offers an innovative way of testing a material in structural engineering.

3. METHODOLOGY

Figure 1 shows the theoretical framework used in this study. A preliminary mix design for geopolymer mortar was conducted in order to identify an optimal mortar mixture among the experimental batches of geopolymer mortar with silica fume and varying amounts of potassium hydroxide and sodium hydroxide. A compressive strength test was conducted, and this parameter with the highest value was used as an indicator for the optimum batch mixture. The optimized geopolymer mixture served as a control for comparison with geopolymer mortars containing varying amounts of polypropylene fiber and bacteria. Bacillus subtilis and Bacillus megaterium bacteria were chosen, each at a concentration of $1.5x10^8$ cells/mL. Pre-cracking of the mixtures occurred on the 28th day at a rate of 1.2 kN per second. Following a 14-day healing period in a water-cured environment, all mixtures underwent post-crack evaluation. Pre-cracking and post-cracking evaluations were conducted to assess the healing potential of the geopolymer batch mixtures, and self-healing percentage was used as an indicator for the selection of the optimum batch to be used in masonry walls as infill material.

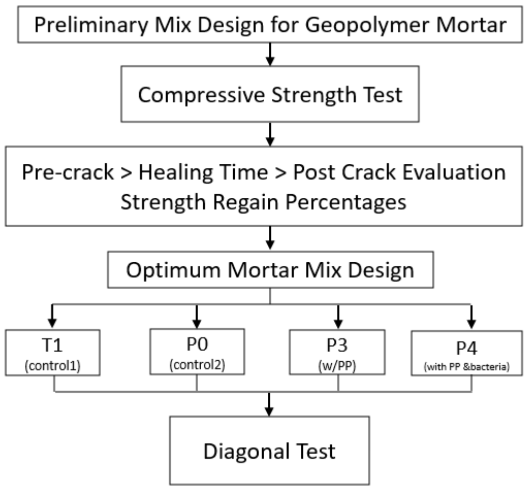

Fig.1 Theoretical framework

Four (4) batches of masonry wallettes in triplicates were fabricated, in which one batch (T1) represents the trial batch in order to determine the ultimate shear capacity of the wallettes for pre-cracking. Pre-cracking of the masonry wallettes occurred on the 14th day at a rate of 5 mm/min. Digital Image Correlation (DIC) was employed to monitor vertical displacement changes in the wallets compared to the Linear Variable Displacement Transducer (LVDT) method. The bacteria were directly added to the geopolymer mortar mix. Following a 14-day healing period in a water-cured environment, all the unreinforced masonry (URM) wallettes underwent post-crack evaluation. The strength-regain ratio was then calculated by subjecting all the URM wallettes to diagonal testing until failure.

3.1 Batch Formulation

The results of a prior study by Quiatchon et al. [20] were used for the batch formulation of the geopolymer mortar and Grino et al. [21] for the application of the geopolymer mortar (with and without bacteria) as infill for masonry wallettes. Bacillus subtilis and Bacillus megaterium were the two types of bacteria used, and they were acquired from the University of the Philippines Los Baños (UP LB) Biotech National Institute of Molecular Biology & Biotechnology.

3.2 Preparation of Geopolymer Mortar and URM Wallet Assembly

Raw materials were weighed and the alkaline solutions were then prepared. Fly ash and sand were mixed in a pan using manual mixing. This was followed by mechanical mixing using JJ-5 cement mortar mixer with water and the pre-prepared alkaline solution (including sodium hydroxide, potassium hydroxide, and sodium silicate solution). The mixed geopolymer mortar was then cast into two sets of 50 mm x 50 mm x 50 mm polyethylene molds, each containing three cube compartments. Following a 24-hour curing period in the mold, the specimens were carefully demolded and stored in a controlled environment for further curing. To maintain moisture within the geopolymer matrix, each demolded cube was wrapped entirely in plastic cling wrap. The ASTM C109/C109M standard guided the casting process, quality control procedures, and subsequent unconfined compressive strength (UCS) testing.

The average ultimate compressive strength and strength regain percentages of the geopolymer mortar specimens in triplicates were determined. From the eight (8) batches of geopolymer mortar, PP3 (Geopolymer mortar with 0.75% polypropylene fibers) and BP3 (Geopolymer mortar with 0.75% polypropylene fibers and bacteria) were considered as the optimum geopolymer mixtures since it yielded a maximum compressive strength and strength regain percentages for the two separate batches. These geopolymer batches were utilized as infill materials for the unreinforced masonry wallettes.

The unreinforced masonry (URM) wall assembly is constructed using clay bricks and geopolymer mortar as the infill material. The dimensions of each unreinforced masonry wallete were 295 mm × 295 mm × 40 mm made of two types of bricks, as shown in Figure 2. This setup is similar to the one used by Umair et al. [22] for scaled-down masonry panels and bricks. The two types of bricks were arranged in a running bond pattern within a 295 mm x 295 mm x 40 mm formwork constructed from sintra boards to form a masonry wallete layer. The first brick is 75 mm x 38 mm x 50 mm, and the second brick is 56 mm x 38 mm x 50 mm. Geopolymer mortar is poured into the formwork with the laid bricks to form the URM masonry wallete with 10 mm mortar thickness.

A trial wallette in triplicate was made and tested for diagonal shear, and this served as baseline data for the ultimate shear strength of the masonry wallettes. A total of twelve (12) masonry wallettes were fabricated, and six (6) masonry wallettes were subjected to preloading of 50% ultimate capacity in the diagonal shear test, and the other six (6) were used as the control. The basis for setting the 50% preloading value was derived from Gupta et al. [23], who used 50% and 70% preloading values to investigate the strength regain of microfibers and superabsorbent polymers in mortar. After fabricating the masonry wallettes with geopolymer mortar as infill material, an ambient curing period of 14 days was used. This is the same curing period used by Wang et al. [24] for masonry walls. Lastly, a comparison of vertical displacement was conducted in the masonry wall using the linear variable differential transformer (LVDT) and digital image correlation (DIC) methods based on the diagonal test results.

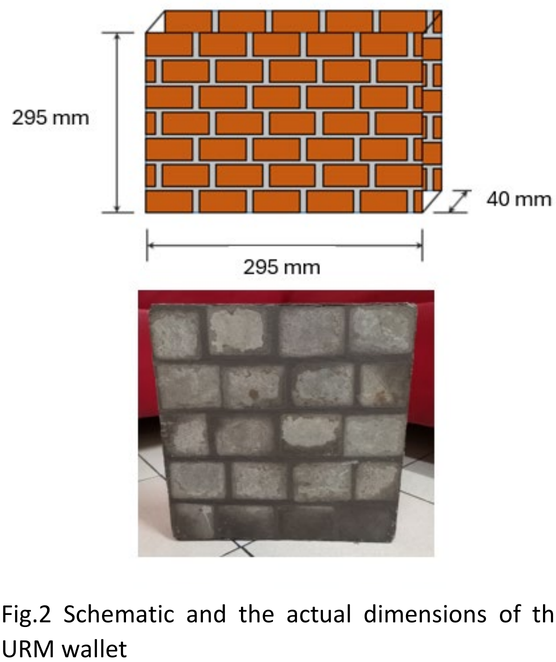

Fig.2 Schematic and the actual dimensions of the URM wallet

Table 1 Batch code description and designation of the masonry wall panels

Code	Description	Number of specimens	Batch naming
T1	Control wallette without PP	3	T1a to T1c
P0	Control wallette with PP	3	P0a to P0c
P3	Wallette with PP (pre-crack)	3	P3a to P3c
P4	Wallette with PP and bacteria (pre-crack)	3	P4a to P4c
	Total	12	

Table 1 outlines the batch code designations for the masonry wall panels. Panel T1 and P0 served as the control, comprising unreinforced masonry bricks with a full coverage geopolymer mortar infill. Panel P3 was a pre-cracked panel constructed with clay bricks and geopolymer mortar with polypropylene fiber as infill material. Similarly, Panel P4 was pre-cracked, but its infill material was a geopolymer mortar containing bacteria and polypropylene fiber.

3.3 Test Procedure

3.3.1 Diagonal Shear Test

Following ASTM E519 standards, the diagonal shear strength of the wall panels was evaluated using a Shimadzu Universal Testing Machine (Model AG-100kNXplus) with a 50 kN capacity. The test was conducted at a displacement-controlled rate of 5 mm/min. During testing, a load cell measured the applied force, while linear variable differential transformers (LVDTs) tracked the displacements parallel and perpendicular to the loading direction. An Almemo data logger from Ahlborn acquired data from both the load cell and LVDTs. This test method simulates diagonal cracking in real-world scenarios by compressing the wall panels until they fail in diagonal tension, splitting apart along the direction of the force. It can be seen in Figure 3 the actual diagonal testing of the wall panel.

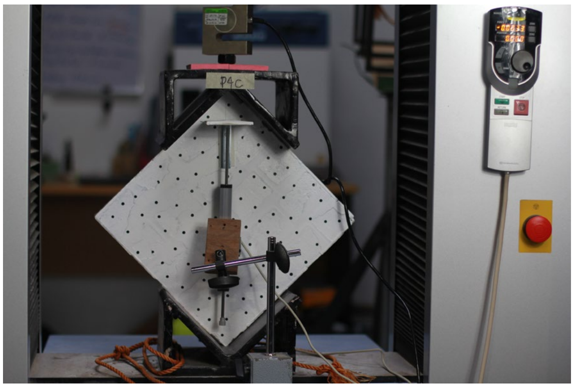

Fig.3 Masonry wallette with a specimen code P4c subjected to a diagonal test

The upper and lower loading shoes were positioned to be centered on the upper and lower bearing surfaces of the testing machine. The load was applied at a uniform rate. The shear stress, net area, shear strain, and modulus of rigidity of the specimen were calculated by applying Equations 1–4.

$$S_s = \frac{0.707P}{A_n} \quad (1)$$

where Ss is the shear stress on net area in MPa, P is the applied load in Newton, and An is the net area of the specimen in square mm.

$$A_n = \left(\frac{w+h}{2}\right) t_n \quad (2)$$

where w is the width of the specimen in millimeters, t is the total thickness of the specimen in millimeters, h is the height of the specimen in millimeters, and n is the percent of the gross area of the unit expressed as a decimal.

$$\gamma = \frac{\Delta V + \Delta H}{g} \quad (3)$$

where γ is the shearing strain (mm/mm), ΔH is the horizontal extension in millimeter, ΔV is the vertical shortening in millimeter, and g is the vertical length in millimeter.

$$G = \frac{S_s}{\gamma} \quad (4)$$

where G is the modulus of rigidity in MPa.

The strength regain ratio quantifies the material's ability to restore its load-bearing capacity after the healing period. It can be computed by taking the ratio of strength after healing to the original strength before cracking, expressed as a percentage, as shown in Equation 5, which was adapted from Xu et al. [25].

$$r_R(\%) = \left(\frac{R_{sh}}{R_f}\right)x100 \quad (5)$$

where Rsh is the strength (compressive/diagonal shear strength) in MPa after the healing period and Rf is the strength (compressive/diagonal shear strength) at first loading (MPa).

3.3.2 Digital Image Correlation (DIC)

All the relevant images were taken using a digital camera (Canon 60D, 18 MP APS-C CMOS sensor, 5.3 fps) in order to determine how the masonry wallets would deform under the actual diagonal test as shown in Figure 4. Prior to testing, the masonry wallets were painted white in preparation for the speckle pattern. Using a black pentel pen marker, a speckle pattern with black dots was randomly generated on one side of the wallet. An open-coded Ncorr software was used to process the digital image correlation of all the images captured during the diagonal test. This is the same software that other researchers used to observe the deformation behavior and interpret the strain analysis of the material [26-30]. By comparing the relative locations of the black dots before and after the testing, the built-in algorithm in the Ncorr software can process all the raw images and determine the deformation behavior of the masonry material.

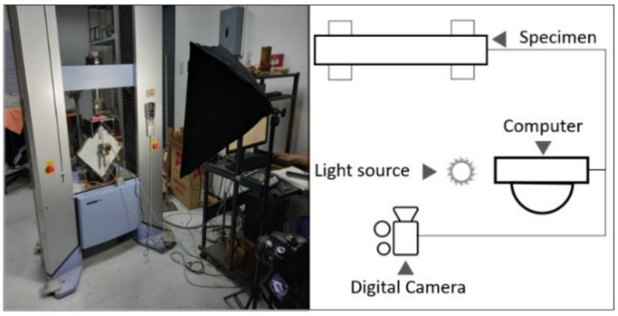

Fig.4 Schematic and actual setup for Diagonal Test with Digital Image Correlation (DIC)

4. RESULTS AND DISCUSSION

4.1 Diagonal Test

Diagonal Shear Test was conducted in order to determine the diagonal tensile or shear strength of masonry walletes by loading them in compression parallel to the diagonal side of the material. A total of nine (9) walletes were fabricated and tested using the Universal Testing Machine (UTM) with a displacement rate of 5 mm/min in accordance with ASTM E519.

Table 1. Result of Diagonal Shear Test of Masonry Walletes

Batch code	Max load (kN)	Shear stress (MPa)	Strength regain ratio (%)
P0 (control)	41.08±10.81	2.46±0.65	--
P3 (no bacteria)	38.07±7.86	2.28±0.47	186.23±40.14
P4 (w/bacteria)	46.19±3.48	2.77±0.21	225.39±21.29

± Confidence Interval (95%)

As shown in Table 1, the result of the diagonal test of three masonry walletes in triplicates showing a range of 38.07 to 46.19 kN compression load and 2.28 to 2.77 MPa shear stress. The P4 batch (masonry wallets with bacteria) obtained the highest load of 46.19 ± 3.48 kN (95% CI) with a shear stress of 2.77± 0.21 MPa (95% CI). It was observed that a percentage increase of 12.44% in maximum load and 12.60% in shear strength of P4 relative to the control.

The average ultimate load of P0(control) masonry wallet was used as control to pre-crack the other wallets by 50% of the ultimate capacity. Following a 14-day healing period, the walletes were carried out to another diagonal test to establish the ultimate load and shear stress of the walletes. It can be observed that a regain strength of 225.39 ± 21.29 % in P4 and 186.23 ± 40.14% in P3 masonry walletes. This only proves that the direct addition of bacteria to fly-ash based geopolymer with polypropylene fibers can be used as an alternative method to repair and strengthen the masonry walletes. This is the same finding as that of Al-Fakih et al. [31], who found out that geopolymer concrete may be effectively healed by adding bacteria directly to the mixture without the need for encapsulation or immobilization methods.

4.2 Mode of Failure

All masonry wallettes exhibited a characteristic diagonal shear failure, leading to the complete collapse of the masonry wall material. This finding corroborates previous research by Mahmood and Ingham [32], which demonstrated crack propagation along the direction of the load. Given the aspect ratio (H/L) of 1.0 of the walls, the anticipated mode of failure, as suggested by Nazir [16], was either diagonal cracking or base sliding. Cracks traversed through various components, including infill geopolymer mortar, clay bricks, or both.

Fig.5 P0c wallet specimen showing the diagonal cracks after the test

Fig.6 P3b wallet specimen showing the diagonal cracks and sliding shear failure of the material

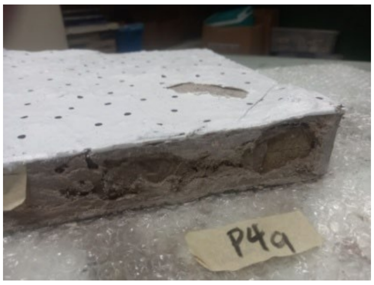

Fig.7 P4a wallet specimen showing the diagonal cracks after the test

P0 and P4 displayed a classic diagonal shear failure as shown in Figures 5 and 6, with cracks extending into the clay bricks, emphasizing the robust interlocking pattern. Additionally, tensile brick failure was observed, indicating strong brick-mortar adhesion. Conversely, P3b experienced a combination of diagonal and sliding shear failure, as illustrated in Figure 6.

4.3 Digital Image Correlation (DIC) result

Using Ncorr software in Matlab, the results of the Digital Image Correlation (DIC) was obtained for the three walletes masonry specimens. The DIC analysis was performed by selecting the reference image, setting the region of interest and other parameters. A total of six (6) images were selected for each wallettes with one reference image. It can be seen in Figures 8 -10 the result of the DIC analysis for the vertical displacement and the median value was used to represent the vertical displacement of the masonry wall.

Table 2. Comparison between LVDT and DIC method in measuring the vertical deformation

Specimen code	LVDT (mm)	DIC (mm)	Percent Difference (%)
P0a	5.65	4.57	19.12
P3b	10.32	9.03	12.50
P4b	7.53	6.05	19.65
Average			17.09

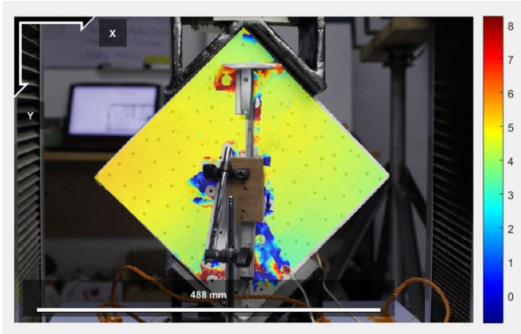

Fig.8 Digital Image Correlation (DIC) result for the vertical displacement of P3b

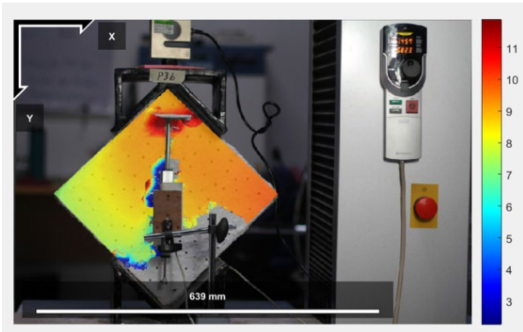

Fig.9 Digital Image Correlation (DIC) result for the vertical displacement of P3b

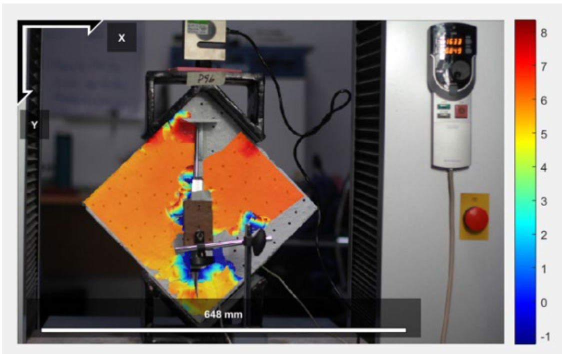

Fig.10 Digital Image Correlation (DIC) result for the vertical displacement of P3b

It can be observed in Table 2, the result of the comparison between LVDT and DIC method. A minimum percentage difference of 12.50% in P3b masonry wallet specimen and a maximum percentage difference of 19.65% in P4b masonry wallet specimen. The average percentage difference between LVDT and DIC is 17.09%. This is consistent with previous studies that investigated at the accuracy of the DIC testing application and discovered that the inaccuracy ranged from 5% to 32% [33] and the results shows a good agreement with the manual measurements [34]. Hence, The Digital Image Correlation (DIC) approach can be utilized as an alternate way to determine the vertical displacement of the material.

5. CONCLUSION

An alternate technique for repairing and strengthening the unreinforced masonry walletes is by using a geopolymer mortar as an infill material with bacteria and polypropylene fibers. The ultimate load capacity of unreinforced wallettes is from 38.07 to 46.19 kN, with an ultimate shear stress value of 2.28 to 2.77 MPa. Incorporating bacteria into an unreinforced brick wallette resulted in an increase of 12.60% in the ultimate shear stress and 12.44% in the ultimate load capacity, with a strength regain value of 225.39%. Hence, the inclusion of bacteria as an infill material in the wall can be a feasible method to repair and strengthen the masonry wallete. By comparing the results of LVDT and DIC, it revealed that Digital Image Correlation (DIC) can be utilized as an alternate approach for evaluating the in-plane behavior of an unreinforced masonry wallette since the percentage difference is 17.09%.

For the DIC, an additional lighting source is recommended in order to capture the raw images and eliminate any possible noise for data processing. Also, it is advisable to adapt a uniform density of speckle patterns to all unreinforced masonry wallettes.

6. ACKNOWLEDGMENTS

The authors would like to acknowledge the BASE Bahay Foundation, Inc. for material wall testing and the Department of Science and Technology - Engineering Research and Development for Technology (DOST-ERDT) for scholarship and funding the experiment.

7. REFERENCES

1. Zengin, B. and Kocak, A., The effect of the bricks used in masonry walls on characteristic properties. Sigma Journal of Engineering and Natural Sciences, Vol. 35, Issue 4, 2017, pp. 667-677. https://izlik.org/JA36KE43CM.
2. Albitar, M., Ali, M., and Visintin, P., Experimental study on fly ash and lead smelter slag-based geopolymer concrete columns. Construction and Building Materials, Vol. 141, 2017, pp. 104–112. https://doi.org/10.1016/j.conbuildmat.2017.03.014.
3. Zhang, P., Zheng, Y., Wang, K., and Zhang, J., A review on properties of fresh and hardened geopolymer mortar. Composites Part B Engineering, Vol. 152, 2018, pp. 79–95. https://doi.org/10.1016/j.compositesb.2018.06.031.
4. Vasconcelos, G., and Lourenço, P. B., Experimental characterization of stone masonry in shear and compression. Construction and Building Materials, Vol. 23, Issue 11, 2009, pp. 3337–3345. https://doi.org/10.1016/j.conbuildmat.2009.06.045.
5. Menon, A., and Magenes, G., Definition of seismic input for out-of-plane response of masonry walls: I. Parametric study. Journal of Earthquake Engineering, Vol. 15, Issue 2, 2011, pp. 165–194. https://doi.org/10.1080/13632460903456981.
6. Sisti, R., Corradi, M., and Borri, A., An experimental study on the influence of composite materials used to reinforce masonry ring beams. Construction and Building Materials, Vol. 122, 2016, pp. 231–241. https://doi.org/10.1016/j.conbuildmat.2016.06.120.
7. Facconi, L., Minelli, F., and Giuriani, E., Response of infilled RC frames retrofitted with a cementitious fiber-mesh reinforced coating in moderate seismicity areas. Construction and Building Materials, Vol. 160, 2018, pp. 574–587. https://doi.org/10.1016/j.conbuildmat.2019.117133.
8. Righetti, L., Edmondson, V., Corradi, M., and Borri, A. Fiberglass grids as sustainable reinforcement of historic masonry. Materials, Vol. 9, Issue 6, 2016, pp. 603-619. https://doi.org/10.3390/ma9070603.
9. Liu, J., Liu, M., and Song, Y. Experimental investigation on flexural performance of masonry walls reinforced with GFRP. Journal of Wuhan University of Technology-Mater Sci Ed, Vol. 22, 2007, pp. 82–84. https://doi.org/10.1007/s11595-005-1082-6.
10. Ferrara, G., Caggegi, C., Martinelli, E., and Gabor, A. Shear capacity of masonry walls externally strengthened using Flax-TRM composite systems: Experimental tests and comparative assessment. Construction and Building Materials, Vol. 261, 2020, pp. 120490-120503. https://doi.org/10.1016/j.conbuildmat.2020.120490.

11. Mustafaraj, E., Yardim, Y., Corradi, M., and Borri, A., Polypropylene as a retrofitting material for shear walls. Materials, Vol. 13, Issue 11, 2020, pp. 2503-2524. https://doi.org/10.3390/ma13112503.
12. Junias, J., and Nayak, S., Augmenting masonry impact resistance: Experimental investigation and statistical reliability assessment. Engineering Structures, Vol. 348, 2025, pp. 121821-121842. https://doi.org/10.1016/j.engstruct.2025.121821.
13. Elmalyh, S., Bouyahyaoui, A., Cherradi, T., Rotaru, A., and Mihai, P., In-plane shear behavior of unreinforced masonry walls strengthened with fiber reinforced polymer composites. Advances in Science, Technology and Engineering Systems Journal, Vol. 5, Issue 2, 2020, pp. 360–367. https://doi.org/10.25046/aj050247.
14. Banerjee, S., Nayak, S., and Das, S., Improving the in-plane behavior of brick masonry wallet using PP band and steel wire mesh. Journal of Materials in Civil Engineering, Vol. 32, Issue 6, 2020. https://doi.org/10.1061/(ASCE)MT.1943-5533.000315.
15. Brunner, J. D., and Shing, P. B. Shear strength of reinforced masonry walls. TMS Journal of Composite Materials, Vol. 14, Issue 1, 1996, pp. 65–77. https://doi.org/10.70803/001c.140460.
16. Nazir, S., Studies on the failure of unreinforced masonry shear walls [Doctoral dissertation, Queensland University of Technology], 2015. https://eprints.qut.edu.au/82792/1/Shahid_Nazir_Thesis.pdf.
17. Manzouri, T., Schuller, M. P., Shing, P. B., and Amadei, B., Repair and retrofit of unreinforced masonry structures. Earthquake Spectra, Vol. 12, Issue 4, 1996, pp. 903–922. https://doi.org/10.1193/1.1585916.
18. Garciano, L., Assessment of strength parameters of URM blocks in heritage structures in the Philippines. International Journal of GEOMATE, Vol. 17, 2019, pp. 61–70. https://doi.org/10.21660/2019.61.4683.
19. Binda, L., Baronio, G., and Tiraboschi, C., Repair of brick masonries by injection of grouts: Experimental research. Journal of Structural Engineering (Madras), Vol. 20, 1993, pp. 29–44. https://doi.org/10.1016/S0950-0618(97)00031-7.
20. Quiatchon, P. R. J., Dollente, I. J. R., Abulencia, A. B., Libre, R. G. D. G., Jr., Villoria, M. B. D., Guades, E. J., Promentilla, M. A. B., and Ongpeng, J. M. C., Investigation on the Compressive Strength and Time of Setting of Low-Calcium Fly Ash Geopolymer Paste Using Response Surface Methodology. Polymers, Vol. 13, Issue 20, 2021, pp. 3461-3478. https://doi.org/10.3390/polym13203461.
21. Griño, A. A., Jr., Soriano, H. S. P., Promentilla, M. A. B., and Ongpeng, J. M. C., Exploring the Potential of Polypropylene Fibers and Bacterial Co-Culture in Repairing and Strengthening Geopolymer-Based Construction Materials. Buildings, Vol. 13, Issue 10, 2023, pp. 2668-2688. https://doi.org/10.3390/buildings13102668.
22. Umair, S., Numada, M., Amin, M., and Meguro, K., Fiber reinforced polymer and polypropylene composite retrofitting technique for masonry structures. Polymers, Vol. 7, Issue 5, 2015, pp. 963–984. https://doi.org/10.3390/polym7050963.
23. Gupta, S., Kua, H. W., and Pang, S. D., Healing cement mortar by immobilization of bacteria in biochar: An integrated approach of self-healing and carbon sequestration. Cement and Concrete Composites, Vol. 86, 2017, pp. 238–254. https://doi.org/10.1016/j.cemconcomp.2017.11.015.
24. Wang, C., Forth, J. P., Nikitas, N., and Sarhosis, V., Retrofitting of masonry walls by using a mortar joint technique; experiments and numerical validation. Engineering Structures, Vol. 117, 2016, pp. 58–70. https://doi.org/10.1016/j.engstruct.2016.03.001.
25. Xu, J., Wang, X., Zuo, J., and Liu, X., Self-healing of concrete cracks by ceramsite- loaded microorganisms. Advances in Materials Science and Engineering, Vol. 2018, Issue 1, pp. 1-8. https://doi.org/10.1155/2018/5153041.
26. Barile, C., Casavola, C., and Pappalettera, G., Digital Image Correlation Comparison of Damaged and Undamaged Aeronautical CFRPs During Compression Tests. Materials, Vol. 12, Issue 2, 2019, pp. 249-262. https://doi.org/10.3390/ma12020249.
27. Aydemir, D., Aksu, O., Bardak, T., Yaman, B., Sözen, E., Ümit Yalçın, Ö., Gündüz, G., and Koçan, N., Mechanical characterization and strain analysis applied to the heat treatment of wood materials, by means of digital image correlation. BioResources, Vol. 19, Issue 2, 2024, pp. 3010-3030. https://doi.org/10.15376/biores.19.2.3010-3030.

28. Harilal, R., Vyasarayani, C., and Ramji, M., A linear least squares approach for evaluation of crack tip stress field parameters using DIC. Optics and Lasers in Engineering, Vol. 75, 2015, pp. 95–102. https://doi.org/10.1016/j.optlaseng.2015.07.004.
29. Casado, C., Pablo, L., Martínez, G., Daniel, C., Molina Aldareguía, J.M., Escudero, S., Segurado Escudero, J. and Llorca Martinez, F.J., Application of digital image correlation at the microscale in fiber-reinforced composites. Composites Part A: Applied Science and Manufacturing, Vol. 43, Issue 10, 2012, pp. 1630-1638. https://doi.org/10.1016/j.compositesa.2011.07.014.
30. Casita, C. B., Iranata, D., Suswanto, B., and Matsumura, M., Graphical Representation of Uniaxial Tensile Test Through Digital Image Correlation, International Journal of GEOMATE, 2024. https://doi.org/10.21660/2024.122.4484.
31. Al-Fakih, A., Mahamood, M., Al-Osta, M., and Ahmad, S., Performance and efficiency of self-healing geopolymer technologies: A review. Construction and Building Materials, Vol. 386, 2023, pp. 131571-131592. https://doi.org/10.1016/j.conbuildmat.2023.131571.
32. Mahmood, H., and Ingham, J. M., Diagonal compression testing of FRP-retrofitted unreinforced clay brick masonry wallettes. Journal of Composites for Construction, Vol. 15, Issue 5, 2011, pp. 810–820. https://doi.org/10.1061/(ASCE)CC.1943-5614.0000209.
33. Buck, N. V., Implementation of an Open-Source Digital Image Correlation Software for Structural Testing. DigitalCommons@CalPoly, 2020. https://digitalcommons.calpoly.edu/theses/2215.
34. Aryanto, A., Revolis, M., Oribe, Y., and Yo, H., Application of Digital Image Correlation Method in Rc and Frc Beams Under Bending Test, International Journal of GEOMATE, 2023. https://doi.org/10.21660/2023.101.g12275.